SURFACE TOPOGRAPHY DUE TO CONVECTION IN A VARIABLE VISCOSITY FLUID: APPLICATION TO SHORT WAVELENGTH GRAVITY ANOMALIES IN THE CENTRAL PACIFIC OCEAN

Jian Lin & E.M. Parmentier

Reprinted from

Geophysical Research Letters

Volume 12, Number 6, June 1, 1985

GEOPHYSICAL RESEARCH LETTERS, VOL. 12, NO. 6, PAGES 357-360, JUNE 1985

SURFACE TOPOGRAPHY DUE TO CONVECTION IN A VARIABLE VISCOSITY FLUID: APPLICATION TO SHORT WAVELENGTH GRAVITY ANOMALIES IN THE CENTRAL PACIFIC OCEAN

Lin Jian and E.M. Parmentier

Department of Geological Sciences, Brown University, Providence, RI 02912

Abstract. To examine the topography and gravity anomalies due to mantle convection, we have carried out finite difference calculations of thermal convection in a fluid layer with a viscosity exponentially decreasing with temperature. Both surface topography and gravity anomalies are shown to be positive over regions of ascending flow and negative over regions of descending flow. These results differ significantly from those of McKenzie (1977) which for similar conditions predict negative topography and gravity anomalies above rising plumes. At large Rayleigh number, the amplitude of surface topography is found to depend on Rayleigh number to the seven-ninths power as predicted by boundary layer theory. These results are applied to test the hypothesis that the linear small-scale gravity undulations in the Central Pacific Ocean (Haxby and Weissel, 1983) are caused by convective rolls in a layer at the base of the lithosphere. For a convecting layer thickness one-half the observed gravity wavelength and with plausible values of flexural rigidity and heat flux, we show that convection can produce gravity anomalies of the observed magnitude with a layer viscosity comparable to that determined by post-glacial rebound. However, a large increase of viscosity with depth is required to confine convection to a thin layer. If these anomalies are actively maintained by convective stresses, one possibility is that layered convection may result from compositional stratification of the mantle.

Introduction

Proposed creep laws for the Earth's mantle indicate a rapid decrease in effective viscosity with increasing temperature (e.g. Weertman and Weertman, 1975). A number of studies have already been carried out to investigate the influence of viscosity variation on thermal convection and explore its geophysical implications. We will focus on the possible effects of a temperature-dependent mantle viscosity on surface topography and gravity anomalies due to finite amplitude thermal convection.

Several earlier studies have examined the surface topography and gravity anomalies that would result from convection in a variable viscosity mantle (McKenzie, 1977; Parmentier and Turcotte, 1978). For a convecting layer of constant viscosity fluid, the surface is elevated above regions of ascending flow and depressed above regions of descending flow. However, the study of McKenzie (1977) predicted that the surface would be locally depressed above regions of ascending flow for a strongly temperature-dependent viscosity. If correct, this could have important implications; for example it might explain the presence of an axial valley on slow spreading mid-ocean ridges. To further examine gravity and topography due to convection we present results for two-dimensional periodic modes of convection in a fluid layer with temperature-dependent viscosity. The calculated surface topography as a function of Rayleigh number is compared with that predicted by boundary layer scaling.

Gravity anomalies recovered from SEASAT altimeter data provide the most direct evidence yet presented for small-scale convection beneath the oceanic lithosphere (Haxby and Weissel, 1983). Certain oceanic regions are characterized by small-scale undulations in the gravity field, with the Central Pacific Ocean as the best example. These undulations have 150-250 km wavelengths and 8-20 mgal peak to trough amplitudes. Haxby and Weissel interpreted them as a possible manifestation of small-scale convection in the low velocity zone of the sublithospheric upper mantle. The breakdown of the linear relationship between sea floor depth and the square root of age at about 70 Ma might also be explained by the presence of small-scale convection under old sea floor which transfers heat to the bottom of the plate thus keeping sea floor depth constant (Parsons and McKenzie, 1978). Based on our results, small-scale convection in a layer at the base of the lithosphere that transfers sufficient heat to explain flattening of seafloor with age can also explain the amplitude of the observed gravity anomalies.

Paper number 5L6504.
0094-8276/85/005L-6504$03.00

Thermal Convection and Surface Topography

The basic equations describing thermal convection can be found in numerous earlier studies (e.g. Parmentier, 1975). Convection of a viscous fluid with infinite Prandtl number confined between two horizontal isothermal boundaries is considered. The Boussinesq approximation is adopted so that the effects of compressibility and viscous dissipation are neglected. The governing equations are put in dimensionless form with the Rayleigh number Ra defined in terms of the temperature difference between the top and bottom boundaries and a viscosity evaluated at the mean temperature. The thermal diffusivity and the coefficient of thermal expansion are assumed to be constant, however, the dimensionless viscosity $\eta = \exp[-CT]$ where C is a measure of the temperature dependence of viscosity and T varies between $-1/2$ and $+1/2$ on the upper and lower boundaries, respectively. Since each convection cell in a two-dimensional, horizontally periodic pattern is the mirror image of an adjacent cell, symmetry conditions for vertical velocity, stream function and temperature are prescribed on the vertical boundaries of each cell. For our studies with temperature-dependent viscosity, we take the horizontal boundaries to be shear stress-free.

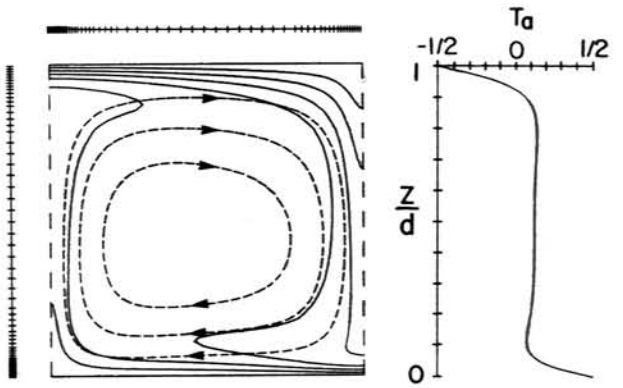

Fig. 1. Left: Isotherms (solid lines) and streamlines (dashed lines) for convection in a fluid with $Ra = 10^5$ and $C = 4$. Grid point locations in the 56×56 grid are shown by tick marks. Right: Horizontally averaged temperature.

The finite-difference approximations employed in this study are described by Parmentier (1975). An example solution is shown in Figure 1. A non-uniform grid was employed which allowed grid points to be concentrated in the thermal boundary layers where large temperature gradients must be resolved. The viscous flow and temperature outside the boundary layers is more uniformly distributed and can be resolved with much larger grid spacing. If grid points were uniformly distributed, more than three times the number of horizontal and vertical grid points would be required to achieve the same overall resolution. Grid points were distributed to provide relatively similar resolution of the top and bottom thermal boundary layers. Comparing solutions on successively refined grids as fine as 56×56 shows that the temperature structure in the boundary layers is well resolved for moderate Ra ($\leq 10^6$). In terms of Nusselt number, Nu, solutions on 28×28 and 56×56 grids have estimated truncation errors of 3% and 1% or less respectively.

Normal stress equilibrium at the top surface of the convecting layer can be represented as $-\varrho g h(x) = -P + \tau_{zz}$ where the normal stress from thermal convection is balanced by the hydrostatic pressure of the excess mass of topography. Here P is fluid pressure due to convection, τ_{zz} is the deviatoric normal stress, $h(x)$ is the topography, and x is horizontal distance along the top boundary. The topography is calculated using finite difference approximations as discussed in Parmentier and Turcotte (1978).

The calculated topography for constant viscosity with $Ra = 3 \times 10^5$ is shown in Figure 2a. For comparison with the results of McKenzie (1977), the separate contributions to the normal stress due to the fluid pressure P and the deviatoric normal stress τ_{zz} are also shown. For constant viscosity these two contributions are both positive above the ascending plume ($x = 0$) and negative above the descending plume ($x = 1$). Therefore, total normal stress is compressive (elevation) over rising flow and tensile (depression) over sinking flow. For constant viscosity, our results appear to be nearly identical to those of McKenzie (1977; Figure 2). Slight differences arise because McKenzie considered a uniform heat flux rather than a uniform temperature lower boundary and defined Ra in terms of heat flux and viscosity at the top boundary. An equivalent value of this Ra can be obtained by multiplying our Ra by Nu/exp[0.5C].

Significant differences between our results and those of McKenzie arise for temperature-dependent viscosity. This previous study presented three examples in which the viscosity variations measured by the ratio of maximum to minimum viscosity were about 11, 35, and 110. As this viscosity ratio increases, the normal stress above the rising plume changes from compression to tension, and consequently the topography changes from elevation to depression (McKenzie, 1977, Figures 8b,9,10). For $Ra = 2.4 \times 10^5$, the surface is elevated for a viscosity ratio of 11 but depressed for viscosity ratio of 35.

For comparison, we chose values of Ra and the viscosity ratio to match those of McKenzie (1977) as closely as possible. As can be seen in Figures 2b and c, our results predict compressive normal stress (elevation) over the rising plume, as for constant viscosity, even at the highest values of Ra and viscosity ratio. According to our calculations, with a Ra of 3×10^5 and a viscosity ratio of 55, the surface remains elevated over the rising plume. The difference between results of the two studies is the magnitude of fluid pressure P. Relative to the magnitude of τ_{zz}, the pressure variations in McKenzie's results appear to be almost exactly twice as large as ours resulting in the topographic depression which his calculations predict. In summary, we did not obtain the previously reported surface depression above the rising plume for any values of Ra and viscosity ratio examined.

Boundary Layer Scaling

In the limit of large Ra, convective motion is vigorous enough to consider the thermal structure of the cell as an

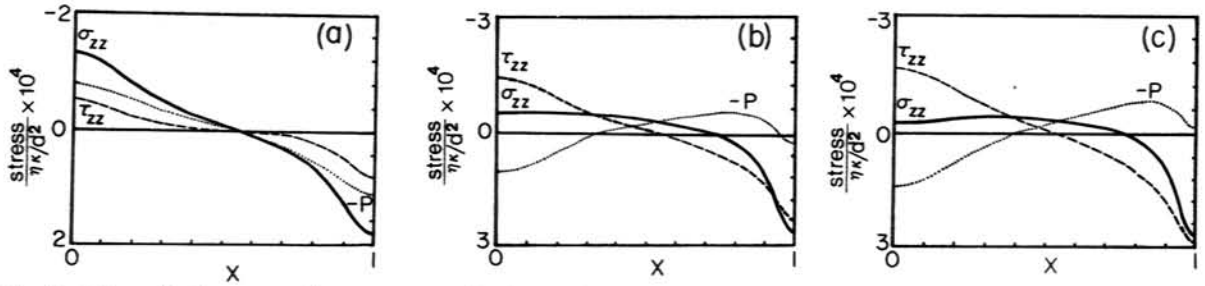

Fig. 2. Dimensionless normal stress σ_{zz} (solid lines), fluid pressure P (dotted lines), and deviatoric normal stress τ_{zz} (dashed lines) on the top boundary of the fluid layer for $Ra = 3 \times 10^5$ with (a) constant viscosity, (b) $C = 4$ or $\eta_{max}/\eta_{min} = 55$, and (c) $C = 5$ or $\eta_{max}/\eta_{min} = 148$. The normalizing viscosity η is that at $T = 0$, $\varkappa$ is the thermal diffusivity, and d is the layer thickness.

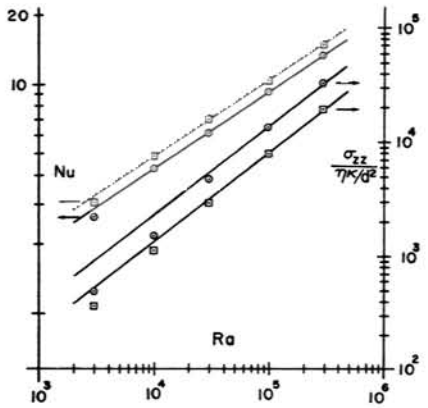

Fig. 3. Nusselt number and normal stress magnitude as a function of Ra for shear stress-free boundaries with constant (squares) and temperature-dependent viscosity (circles) with $\eta_{max}/\eta_{min} = 55$. Calculations for the three highest Ra-values were carried out on 56 × 56 grids like that shown in Figure 1. The two lowest Ra-values are with 28 × 28 grids. Lines represent the boundary layer scaling discussed in the text.

isothermal core enclosed by thin thermal plumes and boundary layers (e.g. Turcotte and Oxburgh, 1967). The fluid motion is driven by buoyancy due to temperature variations in the plumes. For stress-free boundaries, the heat transfer can be characterized by a Nusselt number $Nu \sim Ra^{1/3}$ (Roberts, 1979; Olson and Corcos, 1980). Our numerical results shown in Figure 3 agree closely with this power-law relationship. For no-slip boundaries, Roberts (1979) predicted an exponent of 1/5. For the numerical results in Figure 4, the power-law exponent is between 1/4 and 1/5.

For no-slip and shear stress-free boundaries, the shear stress and horizontal velocity, respectively, on the boundaries depends on $Ra^{2/3}$. However, for both no-slip and stress-free boundaries the dependence of normal stress on Ra is more complicated. As pointed out by Roberts (1979), the Ra-scaling of stresses and velocities near the corners of the cell differ from those in the cell interior. In a corner region of radius r, velocities are proportional to $(RaNu/r)^{1/2}$, where $r \sim Ra^{-2/9}$. This results in a normal stress in the corner regions which depends on $Ra^{7/9}$. The surface topography above the ascending and descending plumes will have this same Ra-dependence. Our numerical results, shown in Figures 3 and 4 agree well with the scaling predicted by boundary layer approximations.

Gravity Undulations and Small-scale Convection

Viscous shearing due to plate motion may cause small-scale convection beneath the oceanic lithosphere to have the form of two-dimensional rolls oriented in the direction of plate motion (Richter and Parsons, 1975). The observed gravity undulations are consistent with convection of this form showing generally periodic variations of relatively constant wavelength in a direction perpendicular to plate motion and being relatively persistent in the direction of plate motion (Haxby and Weissel, 1983). To explain the relatively constant wavelength observed, we consider small-scale convection confined to a layer at the base of the lithosphere. A layer thickness of one-half the wavelength of gravity undulations is assumed since this is approximately the wavelength at which convective instabilites will grow most rapidly. To estimate gravity anomalies as a function of convective heat flux, we use results for a constant viscosity fluid in a layer with no-slip boundaries. For moderate viscosity variation, the magnitude of the normalized topography and the value of Nu are reasonably close to those for constant viscosity (Figures 3). We choose plausible values of other parameters as given by McKenzie, et al. (1974) and a layer thickness of 100 km.

Our model consists of an elastic plate which overlies the convecting layer. Convection exerts a normal stress σ_{zz} on the overlying plate. The vertical deflection of the plate is controlled by its flexural rigidity D and the amplitude and wavelength of the normal stress variation. A flexural rigidity of 2×10^{22} N-m is adopted for Central Pacific Ocean (Forsyth, 1979). The gravity anomaly and heat flux can be calculated if the viscosity and temperature difference across the convecting layer are prescribed. In Figure 5 we plot the amplitude of gravity anomaly as a function of the convective heat flux and viscosity. Isoviscosity lines and lines of constant temperature difference across the layer are shown. The shaded area indicates those combinations of viscosity and temperature difference which lead to Ra less than a critical value of 1707.8. This provides an upper limit on the range of possible viscosity values.

The layer viscosity can be estimated by requiring that the theoretically calculated gravity anomaly and heat flux match those observed in Central Pacific Ocean: peak to trough gravity anomaly 8-20 mgal (Haxby and Weissel, 1983), heat flux 60 mW/m^2 (Sclater and Francheteau, 1970). Since sea floor depth in this part of the ocean is nearly constant, the observed seafloor heat flux is approximately that transferred across the convecting layer. As can be seen in Figure 5, the acceptable values of viscosity are limited to a range from 10^{19} Pa-s to 10^{20} Pa-s with a temperature difference of 300-500°C. Other values could not produce either the observed gravity anomaly or the inferred convective heat flux. This conclusion is not significantly changed by varying the layer depth (75 km to 125 km) or flexural rigidity (10^{22} N-m to 10^{23} N-m).

The viscosity inferred on this basis is very close to that determined from post-glacial rebound studies (Cathles,

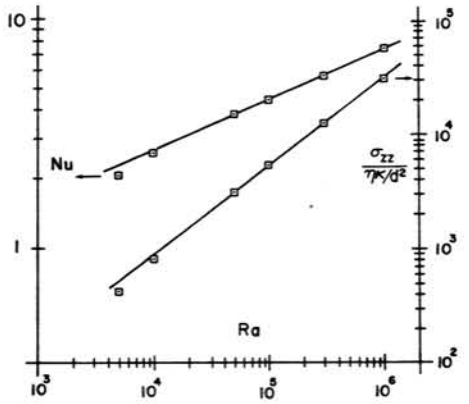

Fig. 4. Nusselt number and normal stress magnitude as a function of Ra for no-slip boundaries and constant viscosity. Calculations were carried out on 28 × 28 grids. Lines represent the boundary layer scaling discussed in the text.

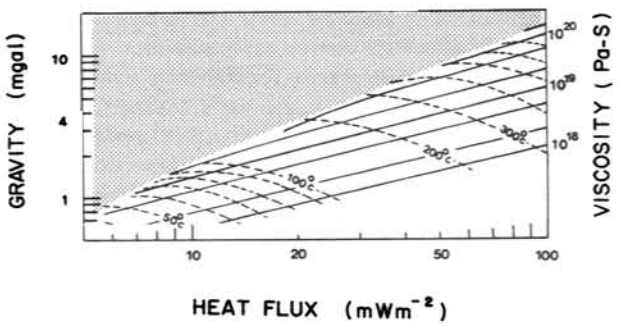

Fig. 5. Gravity anomaly amplitude at sea surface as a function of the heat flux transported by small-scale convection in a 100 km thick layer at the base of the lithosphere. Solid lines show different viscosity values and dashed lines show the temperature difference across the layer. The shaded area represents the combination of viscosity and temperature difference for which the layer is not convectively unstable. Note that a heat flux in the Central Pacific Ocean of about 60 mW/m^2 would produce gravity anomalies with the observed amplitude of 4 to 10 mgals (half the peak to trough value) for a viscosity in the range of 10^{19} to 10^{20} Pa-s.

1975) which predict a value of 5×10^{19} Pa-s in a low viscosity layer beneath the lithosphere. Our conclusion is that for plausible viscosity values, small-scale convection in a layer at the base of the lithosphere can produce the observed gravity anomalies in the Central Pacific Ocean.

However, the viscosity variation with depth inferred from post-glacial rebound or estimated on the basis of laboratory measurements of creep in olivine does not appear to be sufficient to confine small-scale convection to a layer at the base of the lithosphere. Fleitout and Yuen (1984) and Buck and Parmentier (submitted for publication) have also considered small-scale convection in an upper mantle with a temperature and pressure-dependent viscosity consistent with laboratory measurements. The time-dependent models of Buck and Parmentier (submitted for publication) predict that both the horizontal and vertical scale of convective motion increases as the thermal boundary layer thickens with age or distance from the spreading center. To explain the relatively constant wavelength observed, they propose that gravity undulations may result from seafloor topography frozen into the plate at a young age.

If the gravity undulations are dynamically supported by convection, the viscosity beneath a low viscosity zone at the bottom of the lithosphere must be greater than inferred from post-glacial rebound or there must be some other mechanism for confining small-scale convection to a thin layer. Compositional stratification of the mantle is one possibility. Anderson (1984) suggests that a mantle stratification consisting of peridotite overlying a denser eclogite layer beginning at a depth of about 200 km is consistent with models of seismic velocity structure and mineral equation of state data. Alternatively, partial melting of peridotite and the extraction of basaltic magma beneath a mid-ocean ridge should generate a layer of residual mantle which is less dense than the underlying undepleted mantle (Oxburgh and Parmentier, 1977). The thickness of this layer is controlled by the depth to which partial melting extends. If this depth is as large as 150-200 km, a low density depleted layer of the required thickness may result.

Acknowledgements. This paper is based on research supported by the NASA Geodynamics Program under Grant NAG 5-50.

References

Anderson, D. L., The earth as a planet: paradigms and paradoxes, *Science, 223,* 347-355, 1984.

Cathles, L. M., The viscosity of the Earth's mantle, *Princeton Univ. Press,* 386, 1975.

Fleitout, L. and D. A. Yuen, Steady state secondary convection beneath lithospheric plates with temperature- and pressure-dependent viscosity, *J. Geophys. Res., 89,* 9227-9244, 1984.

Forsyth, D. W., Lithospheric flexure, *Rev. Geophys. & Space Phys., 17,* 1109-1114, 1979.

Haxby, W. F. and J. K. Weissel, Evidence for small-scale mantle convection from SEASAT altimeter data, *EOS, 64,* 838, 1983.

McKenzie, D. P., J. M. Roberts, and N. O. Weiss, Convection in the Earth's mantle: towards a numerical simulation, *J. Fluid Mech., 62,* 465-538, 1974.

McKenzie, D., Surface deformation, gravity anomalies and convection, *Geophys. J. R. Astr. Soc., 48,* 211-238, 1977.

Olson, T. and G. M. Corcos, A boundary layer model for mantle convection with surface plates, *Geophys. J. R. Astr. Soc., 62,* 195-219, 1980.

Oxburgh, E. R. and E. M. Parmentier, Compositional and density stratification in the oceanic lithosphere-causes and consequences, *J. Geol. Soc. Lond., 133,* 343-354, 1977.

Parmentier, E. M., Studies of thermal convection with application to convection in the Earth's mantle, Ph.D. thesis, 157 pp., *Cornell University,* 1975.

Parmentier, E. M. and D. L. Turcotte, Two-dimensional mantle flow beneath a rigid accreting lithosphere, *Phys. Earth & Planet. Inter., 17,* 281-289, 1978.

Parsons, B. and D. McKenzie, Mantle convection and the thermal structure of the plates, *J. Geophys. Res., 83,* 4485-4496, 1978.

Richter, F.M. and B. Parsons, On the interaction of two scales of convection in the mantle, *J. Geophys. Res, 80,* 2529-2541, 1975.

Roberts, G. O., Fast viscous Benard convection, *Geophys. Astrophys. Fluid Dynamics, 12,* 235-272, 1979.

Sclater, J. G. and J. Francheteau, The implications of terrestrial heat flow observations on current tectonic and geochemical models of the crust and upper mantle of the earth, *Geophys. J. R. Astr. Soc., 20,* 509-542, 1970.

Turcotte, D. L. and E. R. Oxburgh, Finite amplitude convective cells and continental drift, *J. Fluid Mech., 28,* 29-42, 1967.

Weertman, J. and J. R. Weertman, High temperature creep of rock and mantle viscosity, *Ann. Rev. Earth Planet. Sci., 3,* 293-315, 1975.

(Received March 6,1985;
accepted March 25,1985.)